

NASA TM X-62,406

(NASA-TM-X-62406) VIBRATION-TRANSLATION
ENERGY TRANSFER IN ANHARMONIC DIATOMIC
MOLECULES. 1: A CRITICAL EVALUATION OF THE
SEMICLASSICAL APPROXIMATION (NASA) 30 p HC
\$3.75 CSCL 20H

Unclas
09009

**Ames Research Center
Moffett Field, Calif. 94035**

Vibration-Translation Energy Transfer in Anharmonic
Diatomic Molecules: I. A Critical Evaluation
of the Semiclassical Approximation

Robert L. McKenzie

Ames Research Center, NASA, Moffett Field, California 94035

The semiclassical approximation is applied to anharmonic diatomic oscillators in excited initial states. Multistate numerical solutions giving the vibrational transition probabilities for collinear collisions with an inert atom are compared with equivalent, exact quantum-mechanical calculations. Several symmetrization methods are shown to correlate accurately the predictions of both theories for all initial states, transitions, and molecular types tested, but only if coupling of the oscillator motion and the classical trajectory of the incident particle is considered. In anharmonic heteronuclear molecules, the customary semiclassical method of computing the classical trajectory independently leads to transition probabilities with anomalous low-energy resonances. Proper accounting of the effects of oscillator compression and recoil on the incident particle trajectory removes the anomalies and restores the applicability of the semiclassical approximation.

I. INTRODUCTION

While the collisional excitation of vibrations in diatomic molecules has been a frequently studied topic for decades, present interest in processes that depend on the details of energy transfer to specific vibrational states has put

new demands on the analysis of such collisions. A notable example is the collection of processes occurring in infrared diatomic gas lasers. In many of the recent devices, operating at near-atmospheric densities, a major mechanism for the loss of vibrationally excited molecules is through vibration-translation energy transfer. The rates increase with increasing quantum number, making collisional energy transfer for molecules in initially excited vibrational states an important aspect in the analysis of these laser processes.

Past studies of vibrational energy transfer have dealt mainly with harmonic oscillator models initially in the ground state.¹ Typically, a linearized interaction potential between the oscillator and an incident particle is used, and the particle trajectory is assumed to be collinear with the molecular axis. By adopting a semiclassical approximation, exact and convenient analytical solutions for the oscillator transition probabilities are then obtained for any initial state.^{2,3} The inaccuracy of the harmonic oscillator model has been demonstrated by Mies,⁴ however, even for transitions originating from the ground state. Mies found that the use of an anharmonic oscillator potential introduces matrix elements associated with oscillator transitions that are no longer equal on the diagonal. (A harmonic oscillator with an interaction linear in the oscillator coordinate has diagonal matrix elements equal to zero.)¹ The nonzero differences in the diagonal matrix elements allow additional phase differences between the time-dependent oscillator eigenfunctions to be retained during a collision and can lead to large corrections to the harmonic oscillator model. Because the origin of these corrections resides in the unperturbed oscillator eigenfunctions (from which the matrix elements are computed) their effects are not reproduced by the popular practice of simply inserting oscillator eigenenergies, corrected for anharmonicity, into a harmonic oscillator theory. Similar statements can be made about harmonic oscillators but with a nonlinear interaction.

Again, the diagonal matrix elements are nonzero and unequal, but, although their differences are smaller than for an anharmonic oscillator, the additional phase differences modify the coupling between adjacent states and allow multiple-quantum transitions to occur directly. This study examines the characteristics of vibrational energy transfer for oscillators in initially excited states using both an anharmonic Morse oscillator model and an interaction that is nonlinear in all coordinates.

As a first step, this paper evaluates the applicability of semiclassical methods to anharmonic oscillators. The semiclassical approximation of describing the motion of the incident particle classically and the oscillator response quantum-mechanically is attractive because of its analytical and numerical simplicity. Applications of vibrational rate information usually do not require a precise description of the energy transfer at collision energies near the threshold of vibrational excitation; and further, the incident particle de Broglie wavelength associated with higher collision energies is normally much less than the interaction ranges considered. Hence, semiclassical approximations are expected to be suitable.

A well-known weakness of semiclassical theories, however, is the inherent lack of energy conservation. Several methods of compensation have been suggested that aim at interpreting either the classical trajectory energy,⁴ or velocity⁵ in terms of corresponding values averaged over the collision. Comparisons described here between these semiclassical predictions and some exact quantum-mechanical calculations⁶ show that while such an interpretation is necessary to correct the semiclassical predictions, the results are insensitive to the choice of method in the energy range of practical interest.

Regardless of the corrections for energy conservation, the conventional semiclassical treatment fails badly in some cases. The failures appear in the

form of anomalous resonances that occur only in anharmonic oscillator models and are caused by an incomplete account of the oscillator compression and recoil during impact. Within the usual semiclassical framework, the classical trajectory is computed assuming the oscillator to remain in a pure eigenstate having a fixed average separation of its nuclei. In reality, the oscillator is compressed by the impact and enters a mixed-state condition in which the average internuclear separation oscillates with frequency components from each of the excited states. To include this behavior in the semiclassical theory is not equivalent to conserving energy, but it has the effect of introducing an oscillator "feedback" on the classical trajectory. The effect can change the entire nature of the results in some cases. Extremely heteronuclear or anharmonic molecules, such as the hydrogen halides, are in the class strongly affected.

In this paper, the collision geometry is confined to collinear encounters, making possible direct comparisons with the results of reference 6. Calculations have been made of more realistic three-dimensional encounters,^{7,8} but mainly for harmonic oscillators initially in the ground state. The vibrational transition rates are shown to be strongly dependent on the accompanying rotational transition, and the effect is expected to increase for anharmonic oscillators in excited vibrational states. However, for the purpose of evaluating the semiclassical approximation, little would be gained by adding a more complex collision geometry.

In the paragraphs to follow, a multistate semiclassical formulation requiring numerical solution is assembled, that includes modifications of the standard treatment to account for the effect of oscillator response on the classical trajectory. The model is entirely equivalent to the fully quantum-mechanical model in reference 6, except for the classical treatment of the incident particle motion.

The accuracy of a first-order perturbation theory used by Mies^{4b} for anharmonic oscillators is also evaluated. As expected, the first-order theory is suitable only where the transition probabilities are small; but it is also limited to cases where the oscillator feedback effects are negligible. Such cases pertain mainly to heavy homonuclear molecules impacted by lighter collision partners.

II. SEMICLASSICAL MODEL FOR COLLINEAR COLLISIONS

The collinear collision geometry is shown in Fig. 1 for a structureless particle of mass m_a impacting a diatomic heteronuclear molecule with nuclear masses m_b and m_c . The impacted oscillator nucleus m_b extends from the molecular mass center by a distance γr where $\gamma = m_c/(m_b + m_c)$. A three-body center-of-mass reference frame is taken in which the relative collision speed is \bar{u} . (Barred symbols identify the incident particle variables to be evaluated classically and later interpreted as average values.) Except for the notation, this configuration is identical to those used in references 1, 4, and 6.

To remain compatible with the quantum-mechanical calculations of reference 6, the interaction potential is given the simple form

$$V(y) = A e^{-y/L}$$

where L and A are constants. The potential in terms of mass-center and oscillator coordinates becomes

$$V(\bar{x}, r) = A e^{-\bar{x}/L} e^{\gamma r/L} \quad (1)$$

The Hamiltonian for the three-body system is given by

$$\mathcal{H} = \frac{p_o^2}{2\mu_o} + \frac{\bar{p}^2}{2\mu} + V_o(r) + V(\bar{x}, r)$$

where the symbols with subscripts o refer to oscillator quantities and the other symbols denote incident particle variables. The oscillator reduced mass

is $\mu_0 = m_b m_c / (m_b + m_c)$ and the collision reduced mass is $\mu = m_a (m_b + m_c) / (m_a + m_b + m_c)$.

A. The Incident Particle Motion

The application of Ehrenfest's theorem to the incident particle dynamics guides the formulation of its equation of motion with the quantum-mechanically averaged quantities properly included:

$$\begin{aligned}\frac{d\langle \vec{p} \rangle}{dt} &= -\left\langle \frac{\partial \mathcal{H}}{\partial \vec{x}} \right\rangle = -\left\langle \frac{\partial V(\vec{x}, \mathbf{r})}{\partial \vec{x}} \right\rangle \\ \frac{d\langle \vec{x} \rangle}{dt} &= \left\langle \frac{\partial \mathcal{H}}{\partial \vec{p}} \right\rangle = \frac{1}{\mu} \langle \vec{p} \rangle\end{aligned}$$

By separating the total wavefunction according to

$$\Psi(\vec{x}, \mathbf{r}, t) = \phi(\vec{x}, t) \psi(\mathbf{r}, t)$$

and treating the incident particle classically so that

$$\langle \vec{p} \rangle \rightarrow \mu \vec{u} \quad \text{and} \quad \left\langle e^{-\vec{x}/L} e^{\gamma \mathbf{r}/L} \right\rangle \rightarrow e^{-\vec{x}/L} \left\langle e^{\gamma \mathbf{r}/L} \right\rangle$$

the equations of motion for the incident particle combine with Eq. (1) to give

$$\mu \frac{d^2 \vec{x}}{dt^2} = \frac{A}{L} e^{-\vec{x}/L} \left\langle e^{\gamma \mathbf{r}/L} \right\rangle$$

where

$$\left\langle e^{\gamma \mathbf{r}/L} \right\rangle = \int_{-\infty}^{\infty} \psi^*(\mathbf{r}, t) e^{\gamma \mathbf{r}/L} \psi(\mathbf{r}, t) d\mathbf{r} \quad (2a)$$

In the case of the purely repulsive exponential potential used here, the constant A only influences the distance of closest approach, a quantity of no direct consequence to the transition probabilities, and may be removed by the transformation:

$$A \rightarrow \frac{\bar{E}}{V_{kk}} \exp(x_c/L) \quad \text{where} \quad \bar{E} = \frac{1}{2} \mu \vec{u}^2$$

is the semiclassical relative collision energy before interaction. V_{kk} is the time-independent diagonal matrix element defined by

$$V_{kk} = \int_{-\infty}^{\infty} \psi_k^*(r) e^{\gamma r/L} \psi_k(r) dr \quad (2b)$$

and $\psi_k(r)$ is the initial oscillator stationary-state eigenfunction. If a new interaction coordinate is defined as $\bar{z} = \bar{x} - x_c$, the incident particle motion is then described by

$$\mu \frac{d^2 \bar{z}}{dt^2} = \frac{\bar{E}}{L} \mathcal{R} e^{-\bar{z}/L} \quad (3a)$$

where

$$\mathcal{R} \equiv \langle e^{\gamma r/L} \rangle / V_{kk} \quad (3b)$$

The variable \mathcal{R} represents the quantum-mechanical average effect of the oscillator motion on the interaction potential. Note that, in general, $e^{\gamma r/L}$ does not commute with the oscillator momentum operator in \mathcal{H} , causing \mathcal{R} to depend on the instantaneous condition of the oscillator during the collision.

To compute the trajectory classically, the usual practice at this point is to consider the oscillator fixed in its initial pure eigenstate so that $\psi(r,t) \approx \psi_k(r)$. Then $\mathcal{R} \approx 1$ and the classical equation of motion is reduced to the equation for a constant energy trajectory:

$$\mu \frac{d^2 \bar{z}}{dt^2} = \frac{\bar{E}}{L} e^{-\bar{z}/L} \quad (4)$$

Equation (4) can be integrated analytically¹ so that the interaction potential

$$V(t,r) = \frac{\bar{E}}{V_{kk}} e^{-\bar{z}(t)/L} e^{\gamma r/L} \quad (5a)$$

can be written explicitly in terms of time by use of the result:

$$e^{-\bar{z}(t)/L} = \text{sech}^2\left(\frac{\bar{u}t}{2L}\right) \quad (5b)$$

In such an approximation, the transformation parameter x_c becomes the distance of closest approach.

B. The Oscillator Motion

The unsteady motion of the oscillator is treated in the usual way by expanding its time-dependent wavefunction $\psi(r,t)$ in terms of stationary-state Morse oscillator eigenfunctions $\psi_n(r)$ according to

$$\psi(r,t) = \sum_n c_n(t) e^{-i\omega_n t} \psi_n(r) \quad (6)$$

where $\omega_n = E_n/\hbar$ and E_n is the n^{th} state eigenenergy. For the Morse oscillator,⁹ $\omega_n = \omega_e (n + \frac{1}{2}) - \omega_e \chi_e (n + \frac{1}{2})^2$. The wavefunction $\psi(r,t)$ is the solution of the time-dependent Schrödinger equation:

$$i\hbar \frac{\partial \psi(r,t)}{\partial t} = \left[-\frac{\hbar^2}{2\mu_0} \frac{\partial^2}{\partial r^2} + V_0(r) + V(t,r) \right] \psi(r,t) \quad (7)$$

where

$$V_0(r) = D_e \left[e^{-2a(r-r_e)} - 2e^{-a(r-r_e)} \right]$$

The solutions are invariant with the equilibrium separation r_e and it may be set equal to zero. The remaining potential parameters are equated to the familiar spectroscopic constants ω_e and χ_e according to $D_e = (4\chi_e)^{-1}$ and $a = 2\pi\omega_e(2\mu_0\chi_e)^{1/2}$.

The solution of Eq. (7) is reduced in a standard way to a set of linear, coupled differential equations for the expansion coefficients defined in Eq. (6). Denoting

$$V_{nj} = \int_{-\infty}^{\infty} \psi_n^*(r) e^{Yr/L} \psi_j(r) dr \quad (8)$$

and incorporating the form of the interaction potential in Eq. (5a), the coefficients in Eq. (6) vary in time according to

$$i\hbar \frac{dc_n(t)}{dt} = \frac{\bar{E}}{V_{kk}} e^{-\bar{z}(t)/L} \sum_j c_j(t) e^{i(\omega_n - \omega_j)t} V_{nj} \quad (9)$$

The probability that an oscillator, initially in state k at $t = -\infty$ will reside in state n at $t = +\infty$, is then $\bar{P}_{kn}(\bar{E}) = |c_n(\infty)|^2$ with the initial conditions $|c_j(-\infty)|^2 = \delta_{kj}$ where δ_{kj} is a Kronecker delta.

The matrix elements given in integral form by Eqs. (2b) and (8) may be evaluated analytically.^{4,6} If, for convenience of notation, we define $\alpha = \dot{\gamma}/aL$ and $\beta = \chi_e^{-1}$, then^{4,6}

$$V_{nj} = \beta^\alpha \frac{N_n N_j}{a} \frac{\Gamma(\beta - j)}{n!} \sum_{\ell=0}^j (-1)^{\ell+j-n} \frac{\Gamma(1 + \alpha + j - \ell) \Gamma(\beta - \alpha - 1 - j - n + \ell)}{\ell! (j - \ell)! \Gamma(1 + \alpha + j - n - \ell) \Gamma(\beta - 2j + \ell)}$$

where $\Gamma(\xi)$ is the gamma function¹⁰ with argument ξ and the normalization constants are

$$N_m = [a(\beta - 1 - 2m)/\Gamma(\beta - m)]^{1/2}$$

To stay within the maximum exponent constraints imposed by most computers, the evaluation of matrix elements with large indices requires the ratios of gamma functions to be reduced to products of algebraic terms and a residual gamma function with an argument less than unity.¹⁰

C. Coupling of the Oscillator Motion and the Classical Trajectory

The term $e^{-\bar{z}/L}$ in Eq. (9) may be evaluated either from Eq. (5b) or by the coupled integration of Eq. (3). The latter case requires evaluation of \mathcal{R} in terms of the expansion coefficients — a task easily done by combining Eqs. (2) and (6) to give

$$\mathcal{R} = \frac{1}{V_{kk}} \sum_{\ell} \sum_m c_{\ell}^*(t) c_m(t) e^{i(\omega_{\ell} - \omega_m)t} V_{\ell m} \quad (10)$$

where k again denotes the initial state.

Equation (10) characterizes the classical nature of the oscillator motion. The motion will become oscillatory as soon as a mixed-state condition is produced during the collision and will remain so afterward. Near closest approach,

large transient excursions of \mathcal{R} occur, reflecting the oscillator compression and recoil.

D. First-Order Perturbation Solution

From a practical viewpoint, the convenience of an analytical solution warrants even the coarsest assumptions, provided the limits of applicability are understood. This study attempts to confirm those limits for a first-order perturbation analysis applied to anharmonic oscillators in initially excited states. We shall see that the perturbation solutions are quite successful within their intended limits and will serve as a useful approximation in many cases.

An analytical solution of Eq. (9) may be obtained if the motion of the classical particle is described by Eq. (4). For an initial state k , the perturbation method further requires that $|c_k(t)|^2 \approx 1$ and $|c_n(t)|^2 \ll 1$ throughout the duration of the collision. Then only the initial and final states are coupled, allowing Eq. (9) to be written in the integral form:

$$|c_n(\infty)|^2 = \left| \frac{\bar{E}}{\hbar} \frac{V_{nk}}{V_{kk}} \int_{-\infty}^{\infty} \text{sech}^2\left(\frac{\bar{u}t}{2L}\right) \exp\left[\frac{i}{\hbar} \int_0^t \Gamma_{nk}(t') dt'\right] dt \right|^2 \quad (11)$$

with

$$\Gamma_{nk}(t') = \hbar(\omega_n - \omega_k) + (V_{nn} - V_{kk})(\bar{E}/V_{kk}) \text{sech}^2\left(\frac{\bar{u}t'}{2L}\right)$$

Equation (11) may be integrated to give^{4(b)}

$$\bar{P}_{kn}(\bar{E}) = \left| \frac{V_{nk}}{V_{kk}} \frac{2\pi g \mu L \bar{u}}{\hbar \sinh(\pi g)} M(1 + ig, 2, i2\lambda) \right|^2 \quad (12)$$

where

$$g = L(\omega_n - \omega_k)/\bar{u} \quad , \quad \lambda = \frac{\mu L \bar{u}}{\hbar} (V_{nn} - V_{kk})/V_{kk}$$

and $M(1 + ig, 2, i2\lambda)$ is the confluent hypergeometric series with complex arguments. The necessity of complex algebra may be avoided when computing the modulus $|M(1 + ig, 2, i2\lambda)|$ by noting its relation to the Coulomb wavefunction with zero indice.¹⁰ The result is

$$|M(1 + ig, 2, i2\lambda)| = \Phi_0(-g, \lambda) \quad (13)$$

where

$$\Phi_0(-g, \lambda) = \sum_{\ell=1}^{\infty} A_{\ell} \lambda^{\ell-1}$$

with $A_1 = 1$ and $A_2 = -g$. The remaining coefficients are obtained from

$$\ell(\ell - 1)A_{\ell} = -2gA_{\ell-1} - A_{\ell-2}$$

E. Numerical Solution Methods

Solutions to the coupled set of Eqs. (3) and (9) were obtained by first separating Eq. (9) into a separate set for each complex component and adopting the equivalent of a multiple-state, close-coupling approach. Numerical integration was accomplished with a polynomial extrapolation algorithm originally developed by Bulirsch and Stoer¹¹ and given in FORTRAN by Gear.¹² Fifth-order polynomials and a required accuracy of one part in 10^8 seemed to optimize the calculation of a selected test case and allowed a complete encounter to be computed in 200 to 1000 steps, depending on the collision energy and the number of coupled states. Solutions were started with the molecule in a pure eigenstate and with the incident particle at a distance such that the interaction potential had a value 10^{-4} times the estimated value at closest approach. The calculation was terminated at an equal distance after the encounter. All values of $|c_n(t)|^2$ were sufficiently constant at termination. The closure relation $\sum_n |c_n(t)|^2 = 1$ was used throughout the encounter to monitor accuracy. At the maximum collision energies considered, up to 15 levels above and below the initial state were

required to ensure that the solution was unaffected by neglected states. In the energy range where the perturbation theory was successful, as few as two states were adequate. The computing times required to obtain all of the matrix elements and integrate the dynamics of a 12-state model was approximately 0.1 sec per step on a single-precision (14-digit), CDC-7600 computer.

III. AN EVALUATION OF THE SEMICLASSICAL APPROXIMATION

The availability of tabulated results for exact quantum-mechanical calculations⁶ over a broad range of collision parameters provides an excellent opportunity to evaluate the semiclassical approximation in this application. The extent of the examples covered is characterized by the range of the mass parameter $m = m_a m_c / m_b (m_a + m_b + m_c)$. For the cases chosen, m varies from 0.006 for $\text{Br}_2\text{-H}$ collisions to 3.7 for HBr-He collisions. (Reference 6 labels one data set as $\text{Br}_2\text{-H}_2$ but uses a mass parameter corresponding to $\text{Br}_2\text{-H}$.) A full range of oscillator frequency and anharmonicity is also represented. Figures 2a-f compare the predictions of the semiclassical theory and its first-order approximation to a sampling of the results in reference 6 for the homonuclear oscillator cases. The semiclassical transition probabilities are plotted as functions of the normalized initial kinetic energy of the incident particle, $\bar{E}/\hbar\omega_e$. The probabilities from reference 6, hereafter referred to as "exact," are shown at their appropriate total energies, $E_T/\hbar\omega_e$, and at energies displaced according to a symmetrization scheme to be discussed. In the paragraphs to follow, the comparisons in Figs. 2a-f are used to evaluate the validity of several methods of compensating for the lack of energy conservation in the semiclassical approximation and to demonstrate the influence of coupling between the recoiling quantum-oscillator and the classical incident-particle motion.

A. Energy Conservation and the Classical Parameters

The absence of energy conservation in the semiclassical approximation requires an interpretation to be made of the initial relative kinetic energy \bar{E} assigned to the classical trajectory. It may be considered as an effective value, averaged over the trajectory from the true initial value E_k to the final value E_n , when the molecule undergoes a transition from state k to n . If total energy is conserved, E_T , E_k , and E_n are related by

$$E_k + \hbar\omega_k = E_T = E_n + \hbar\omega_n \quad (14)$$

No formal guidelines are available, however, for simply relating \bar{E} to the exact energies E_k and E_n . Perhaps the closest one can come is with the method described in reference 5 where the formulation of a linearized quantum-mechanical approximation is compared to its semiclassical counterpart. Expressions for the transition probabilities given by both approximations become similar if \bar{E} is defined by the average velocity $\bar{u} = (u_n + u_k)/2$. Another approach is taken by Mies⁴ who uses the intuitively appealing arithmetic energy average $\bar{E} = (E_n + E_k)/2$. Combined with Eq. (14), the total energy can then be related to the average energy according to:

$$E_T = \bar{E} + \hbar(\omega_n + \omega_k)/2 \quad (15)$$

where $\hbar(\omega_n + \omega_k)/2$ is the oscillator energy averaged over the transition. Occasionally, even the geometric average $\bar{E} = (E_k E_n)^{1/2}$ has been suggested. Equation (15) was chosen here for the comparisons in Figs. 2a-f, where it is shown to be generally successful. It correlates the predictions of both theories for all initial states, transitions, and mass ratios tested and appears applicable for all energies \bar{E} from threshold up to at least the first probability maximum. Figure 2c shows correlation beyond the first maximum. Note however, that in the cases where the effect of the oscillator motion coupled to

the classical trajectory is distinguishable, the coupling must be included to preserve the accuracy of Eq. (15). (See Fig. 2a for example.) The other averaging methods are no less accurate, however. Table I reveals that all of the averaging methods described give essentially the same results and that, within the range of these comparisons, the best choice cannot be selected. Differences in the three methods (or apparently any other method) will only become distinguishable at values of $E_T \gg \hbar\omega_e$ where, from thermal considerations, E_T is beyond the range of practical interest. From a pragmatic viewpoint, Eq. (15) is attractive because, unlike the other averages, it provides an energy transformation, $E_T - \bar{E}$, independent of \bar{E} and allows the energies E_k or E_n to be written explicitly in terms of \bar{E} with simple algebraic form. These features are convenient for additional manipulation such as thermal averaging.

Figures 2a-f show correlations of the exact and semiclassical predictions for transitions in which the oscillator energy is increased. If Eq. (15) is adopted and the exact probability for a transition $k \rightarrow n$ is denoted $P_{kn}(E_k)$, where E_k is the initial kinetic energy and $\omega_k < \omega_n$, then

$$P_{kn}(E_k) \approx \bar{P}_{kn}(\bar{E}) \quad (16a)$$

with

$$\bar{E} = E_k - \hbar(\omega_n - \omega_k)/2 \quad (16b)$$

An equivalent interpretation of the semiclassical prediction for a transition $n \rightarrow k$, in which the oscillator loses energy, follows from the principle of detailed balance.¹³ In this application where only collinear collisions and transitions among nondegenerate states of the same spin are considered, detailed balance requires that

$$E_k P_{kn}(E_k) = E_n P_{nk}(E_n) \quad (17)$$

The absence of energy conservation is reflected in the semiclassical result

$$\bar{P}_{kn}(\bar{E}) = \bar{P}_{nk}(\bar{E}) \quad (18)$$

so that the interpretation of $\bar{P}_{nk}(\bar{E})$ equivalent to Eq. (16) must be

$$P_{nk}(E_n) = \frac{E_n + \hbar(\omega_n - \omega_k)}{E_n} \bar{P}_{nk}(\bar{E}) \quad (19a)$$

where

$$\bar{E} = E_n + \hbar(\omega_n - \omega_k)/2 \quad (19b)$$

and E_n is now the initial energy.

B. The Influence of Oscillator Response on the Classical Motion

The discussion to this point has been confined to homonuclear molecules. Figures 2a-f indicate that the coupling of oscillator motion and the classical trajectory has a noticeable effect only for the most anharmonic molecule, H_2 , and then only when struck by a relatively heavy particle, He. However, semiclassical calculations for heteronuclear cases are much more sensitive to the oscillator response. In the customary semiclassical formulation, the incident particle dynamics are related only to its distance from the mass-center of the molecule, and no regard is given for the location of the impacted nucleus. (See Eq. (4) for example.) In an extreme heteronuclear case where the impacted nucleus was extended to a distance similar to the distance of closest approach, the incident particle could spatially overlap the impacted nucleus without constraint. Of course, even the approach to this extreme situation signals the failure of the assumptions leading to Eq. (4).

The hydrogen-halides represent examples of diatomic molecules whose heteronuclear properties are sufficient to influence the incident particle motion, with their effects further augmented by the accompanying large anharmonicity. As an example, Fig. 3 illustrates the results for HB_r-H_e collisions where H

is the impacted nucleus. Similar results were obtained for HCl-He and are assumed to be characteristic for all of the hydrogen-halides. Both the semi-classical numerical solutions and analytical theory predict an anomalous resonance at low energy when the classical trajectory is obtained from Eq. (4). The resonance is a combined result of an improper trajectory and the oscillator anharmonicity, since similar calculations treating the molecule as a harmonic oscillator behaved normally and in accordance with corresponding quantum-mechanical solutions.⁶ Considerable care was exercised in verifying the resonance as a real solution of the theoretical model rather than a numerical artifact. The similar behavior of the analytical solution supports the conclusion that the effect is real for the model used. When oscillator motion is included via Eqs. (3) and (10), the resonance disappears and the solution is more in accordance with the quantum-mechanical results for single-quantum transitions. However, multiple-quantum probabilities such as \bar{P}_{02} still display a low-energy anomalous resonance. The interpretation of \bar{E} for single-quantum transitions is also shown to be less accurate but Eq. (15) still performs well near threshold. The results suggest that the interference between the oscillator and the incident particle is not fully accounted for; but if it were, Eq. (15) would apply.

The effects of the oscillator motion are not generated simply by large excursions of \mathcal{R} during the collision. Figure 4 compares the time-dependent variation of \mathcal{R} with and without the effects coupled to the collision dynamics for two extreme cases: (a) H_2 -H collisions, where the excursions of \mathcal{R} are largest, but the effect is negligible; and (b) HBr- H_e collisions, where the excursions are smaller, but a phase shift is introduced in the oscillator motion that severely alters the remaining oscillator response.

C. Applicability of First-Order Perturbation Theory

Figures 2 and 3 amply demonstrate the fact that not only must \bar{P}_{kn} be small for the first-order theory to apply but that the transient motion of the oscillator must also have no significant effect on the collision dynamics. The appearance of a probability maximum is always an artifact of the semiclassical perturbation approximation and signals the inapplicability of the theory. These conclusions are not surprising, but they further constrain the anharmonic oscillator perturbation theory to heavy homonuclear molecules such as N_2 , O_2 , and the halides. First-order perturbation calculations for slightly heteronuclear molecules such as CO also require careful attention. Just as in the case of H_2 , collisions of CO with lighter particles (e.g., CO-He collisions) were unaffected by the oscillator motion. However, perturbation calculations of collisions with heavier particles (e.g., CO-Ar collisions) displayed large errors due to the coupled oscillator motion and also due to an increased coupling of adjacent oscillator states not included in the perturbation approximation. In the CO-Ar case, the perturbation-theory errors were not accompanied by anomalous probability maximums in the energy range of practical interest.

IV. SUMMARY

The semiclassical approximation has been applied to vibrational transitions induced in anharmonic oscillators by collinear collision with inert atoms. Multistate numerical solutions have been compared with exact quantum-mechanical calculations of an equivalent collision model for a wide range of initial molecular states and collision partners. The comparisons allow a comprehensive assessment of the semiclassical approximation for the anharmonic oscillator model. The semiclassical predictions accurately reproduce the quantum-mechanical transition probabilities for all initial collision energies from threshold to at least the first probability maximum if either the semiclassical collision

velocity or energy is interpreted as a simple average of the exact initial and final values. The accuracy of the correlation between both theories is not sensitive to the choice of averaging method.

The semiclassical approximation, in its usual form where the classical trajectory is computed independently, was found to be applicable to heavy homonuclear molecules such as N_2 , O_2 , and the halides on impact with lighter partners. Lighter homonuclear molecules such as H_2 showed poorer agreement when impacted by a heavier collision partner. Heteronuclear anharmonic molecules such as the hydrogen halides displayed anomalous resonances at low energy that do not appear in their harmonic counterparts. The accuracy of the semiclassical approximation for light or heteronuclear anharmonic molecules was significantly improved by coupling the effects of the time-dependent average motion of the recoiling oscillator to the classical trajectory.

A convenient, analytical, first-order, perturbation analysis for anharmonic oscillators was found to be accurate for small transition probabilities, but only if the effects of the oscillator motion on the classical trajectory were unimportant. The analytical approximation is therefore not applicable to significantly anharmonic and heteronuclear molecules and must be applied with care for slightly heteronuclear molecules such as CO.

REFERENCES

- ¹D. Rapp and T. Kassal, Chem. Rev. 69, 61 (1969).
- ²E. H. Kerner, Can. J. Phys. 36, 371 (1958).
- ^{3a}C. E. Treanor, J. Chem. Phys. 43, 532 (1965).
- ^{3b}C. E. Treanor, J. Chem. Phys. 43, 2220 (1965).
- ^{4a}F. H. Mies, J. Chem. Phys. 40, 523 (1964).
- ^{4b}F. H. Mies, J. Chem. Phys. 41, 903 (1964).
- ⁵T. L. Cottrell and J. C. McCoubrey, Molecular Energy Transfer in Gases (Butterworth and Co. Ltd., 1961).
- ⁶A. P. Clark and A. S. Dickinson, J. Phys. B: Atom. Molec. Phys. 6, 164 (1973).
- ⁷C. F. Hansen and W. E. Pearson, Three-Dimensional Collision Induced Vibrational Transitions in Homogeneous Diatomic Molecules, NASA Tech. Rept. R-355 (1970).
- ⁸E. Eastes and D. Secrest, J. Chem. Phys. 56, 640 (1972).
- ⁹P. M. Morse, Phys. Rev. 84, 57 (1929).
- ¹⁰M. Abramowitz and I. A. Stegun, Handbook of Mathematical Functions, NBS AMS 55 (1964) p. 538.
- ¹¹R. Bulirsch and J. Stoer, Num. Math. 8, 1, (1966).
- ¹²C. W. Gear, Numerical Initial Value Problems in Ordinary Differential Equations, (Prentice-Hall, 1971) p. 96.
- ¹³L. D. Landau and E. M. Lifshitz, Quantum Mechanics (Pergamon Press, 1958) p. 432.

TABLE I. A comparison of symmetrization methods applied to anharmonic H_2

Transitions $k \rightarrow n$	$\frac{E_T - \bar{E}}{\hbar\omega_e}$			
	Observed Fig. 2a-b (a)	$\bar{E} = \frac{1}{2} (E_n + E_k)$	$\bar{u} = \frac{1}{2} (u_n + u_k)$ (b)	$\bar{E} = (E_n E_k)^{1/2}$ (b)
0-1	1.0	0.97	0.99	1.01
0-2	1.3	1.41	1.46	1.50
0-3	1.7	1.83	1.94	2.05
2-3	2.7	2.75	2.76	2.78
2-4	3.1	3.14	3.20	3.26
2-5	3.5	3.51	3.65	3.80
5-6	5.0	5.03	5.06	5.08

^aThe observed energy difference between the semiclassical and exact results for a given probability near threshold. The semiclassical results include oscillator feedback.

^bComputed for $\bar{E}/\hbar\omega_e = 6$.

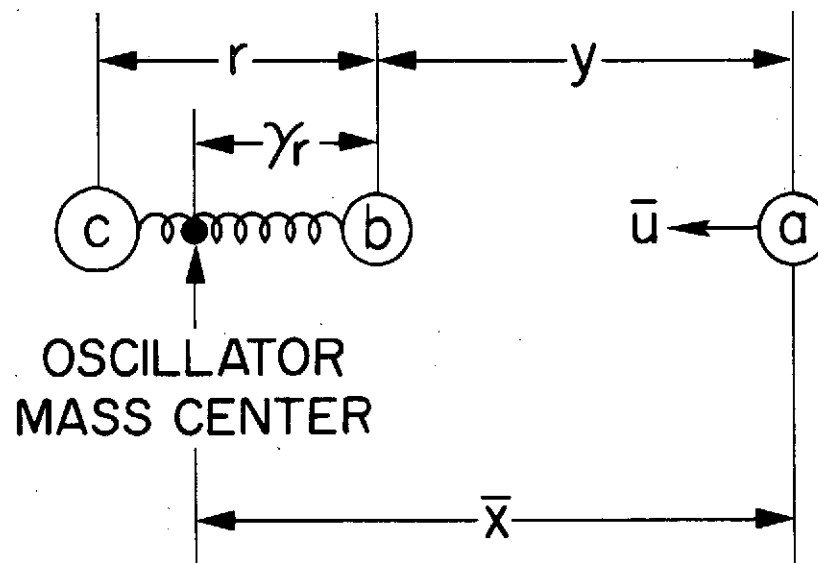
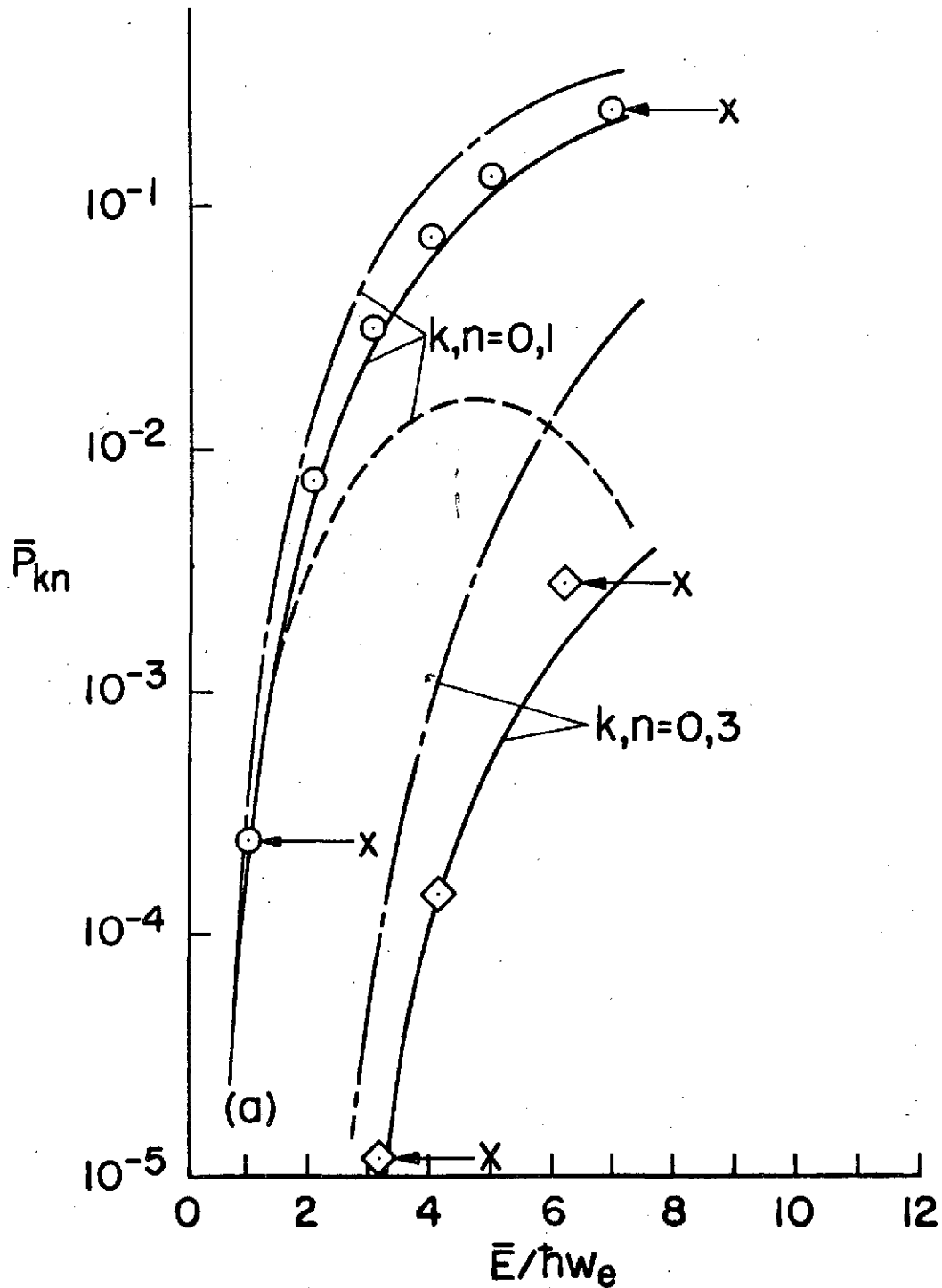


Fig. 1. Colinear collision geometry.



a. $H_2(k=0) - He$ collisions; \circ : $k \rightarrow n = 0 \rightarrow 1$; \diamond : $k \rightarrow n = 0 \rightarrow 3$.

Fig. 2. Comparisons of semiclassical and quantum-mechanical⁶ transition probabilities for homonuclear molecules. All calculations are done for $L = 2 \times 10^{-9}$ cm. Open symbols denote points tabulated in reference 6 and plotted according to Eq. (15). The symbol X locates the value of $E_T/\hbar\omega_e$. The curves — are semiclassical multistate solutions using classical trajectories coupled to the oscillator motion via Eq. (3). The curves — — are the same without coupling via Eq. (4). The curves - - - - are first-order perturbation solutions given by Eq. (12).

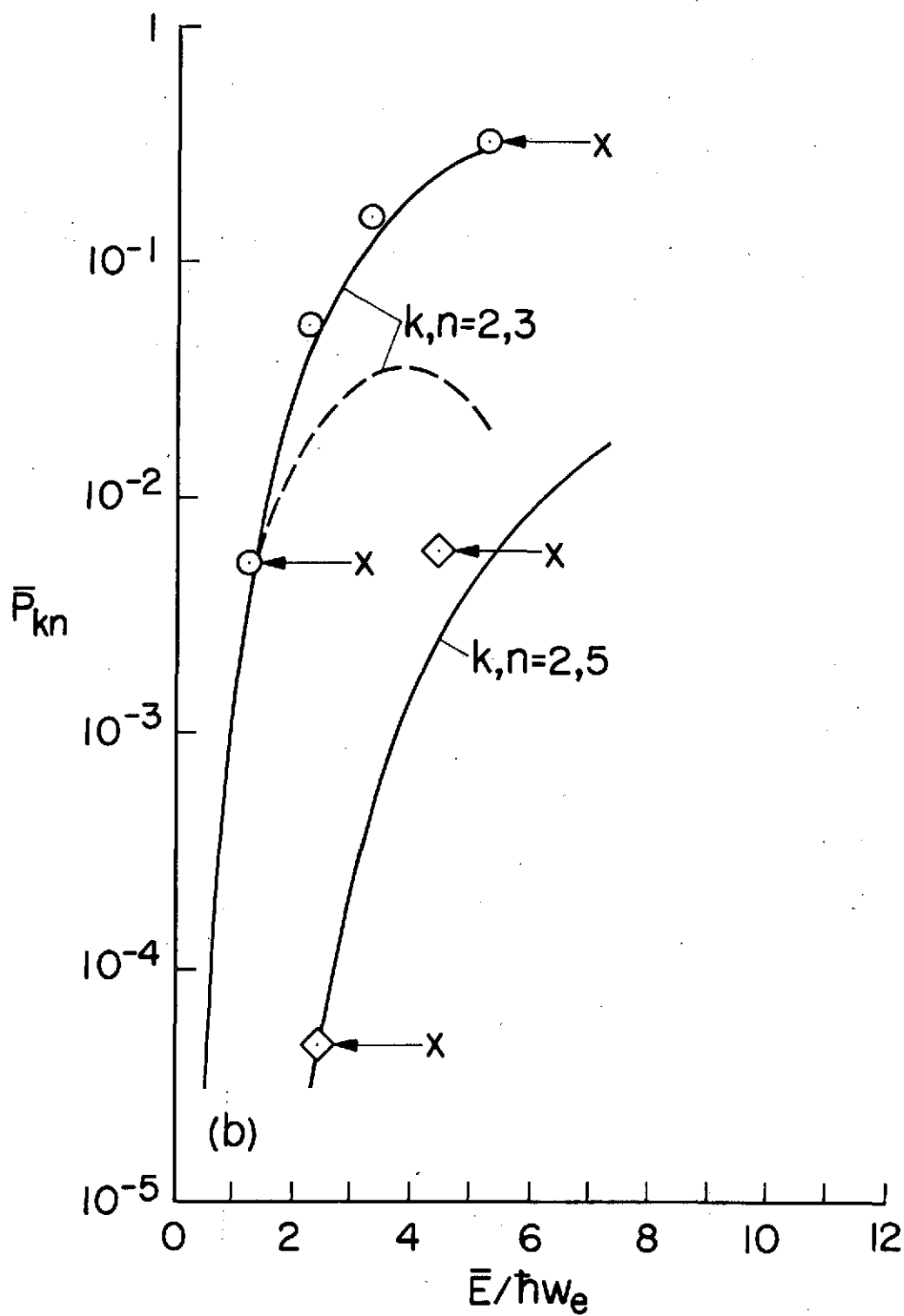


Fig. 2b. $H_2(k = 2) - H_e$ collisions; O: $k + n = 2 + 3$; \diamond : $k + n = 2 + 5$.

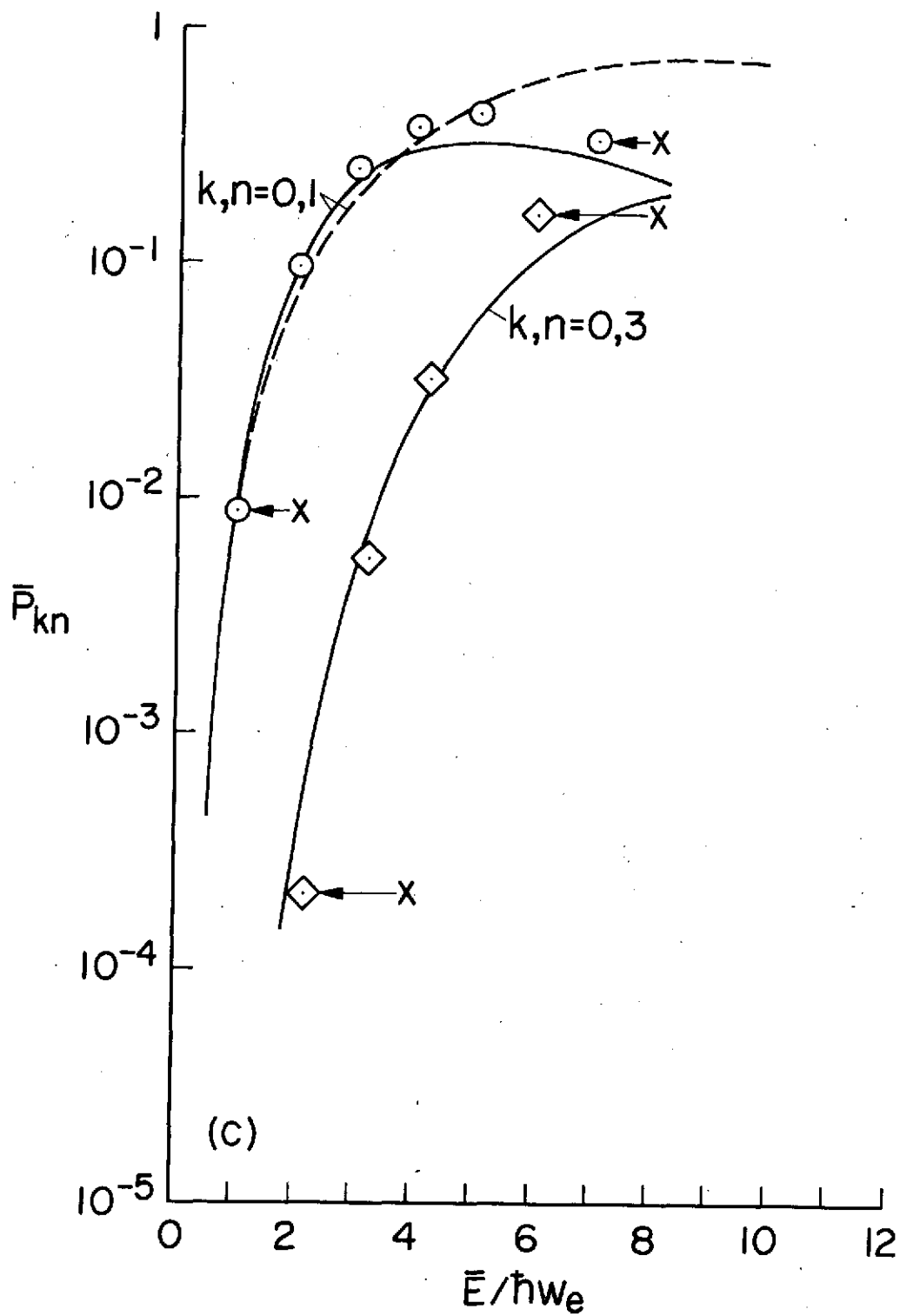


Fig. 2c. $H_2(k=0) - H$ collisions; coupled and uncoupled solutions are superimposed, \circ : $k \rightarrow n = 0 \rightarrow 1$; \diamond : $k \rightarrow n = 0 \rightarrow 3$.

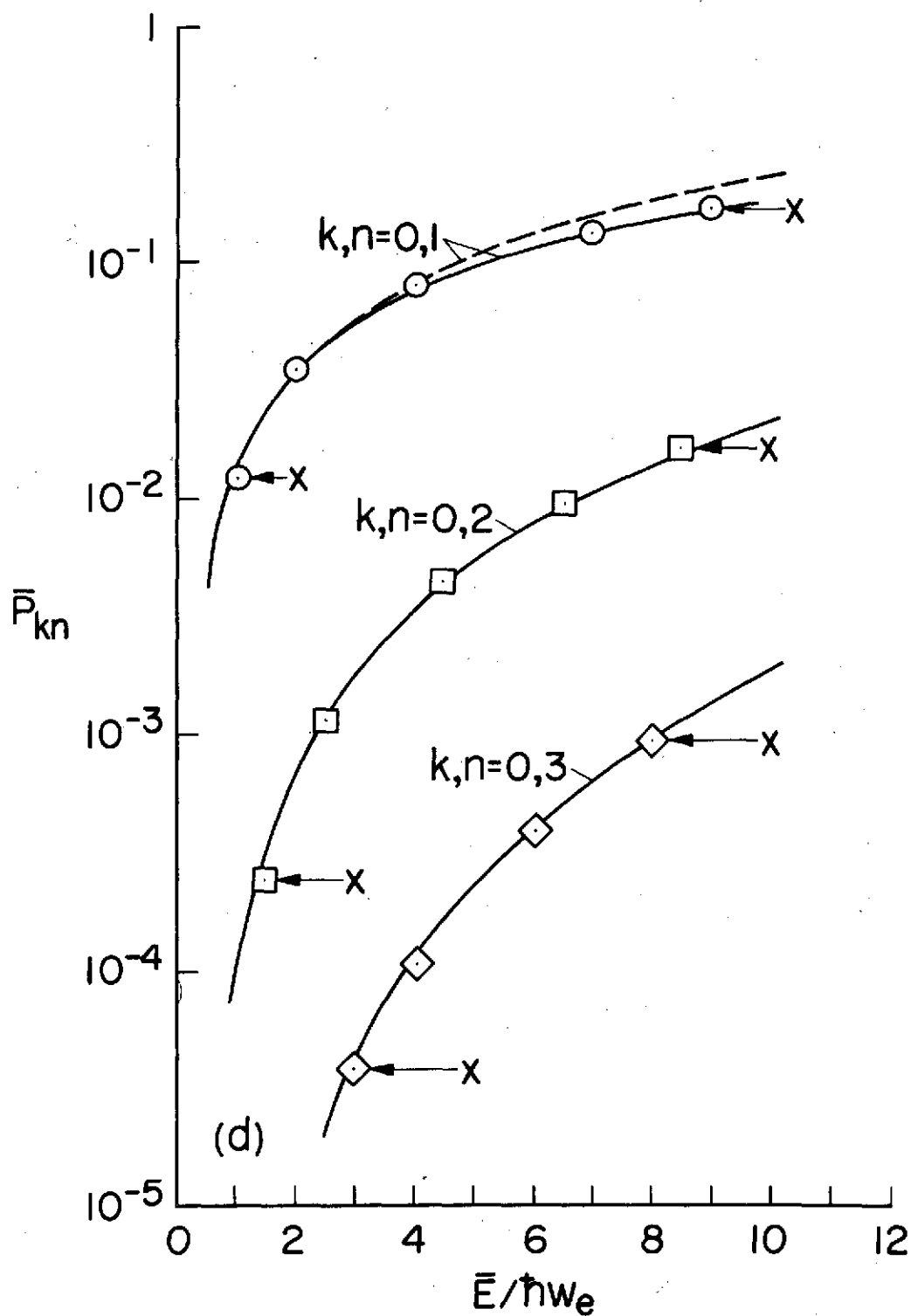


Fig. 2d. $\text{Br}_2(k=0) - \text{H}$ collisions; coupled and uncoupled solutions are superimposed, \circ : $k \rightarrow n = 0 \rightarrow 1$; \square : $k \rightarrow n = 0 \rightarrow 2$; \diamond : $k \rightarrow n = 0 \rightarrow 3$.

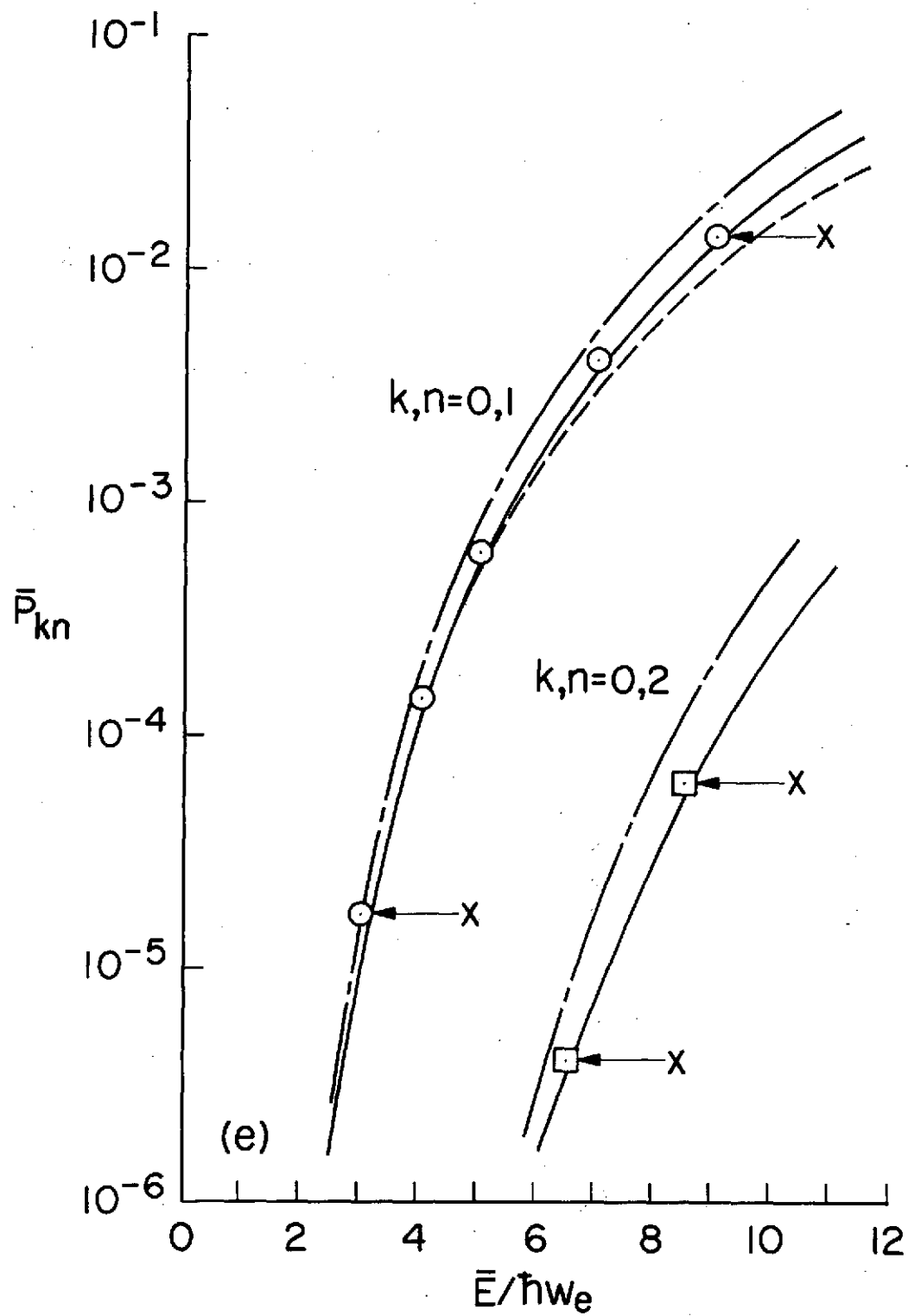


Fig. 2e. $N_2(k=0) - (N_2)$ collisions; O: $k \rightarrow n = 0 \rightarrow 1$; □: $k \rightarrow n = 0 \rightarrow 2$.

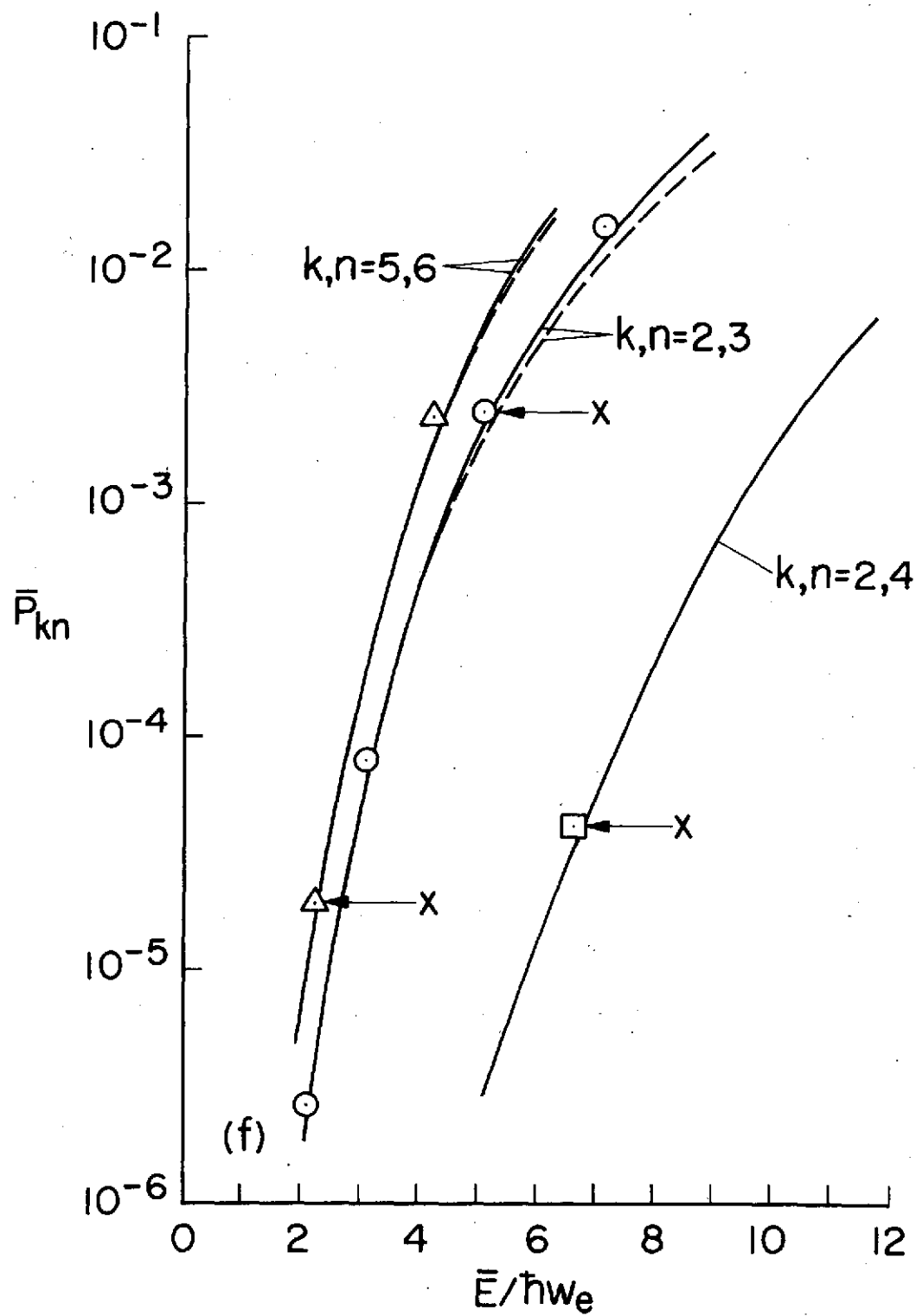


Fig. 2f $N_2(k = 2 \text{ or } 5) - (N_2)$ collisions; O: $k \rightarrow n = 2 \rightarrow 3$; □: $k \rightarrow n = 2 \rightarrow 4$; Δ: $k \rightarrow n = 5 \rightarrow 6$.

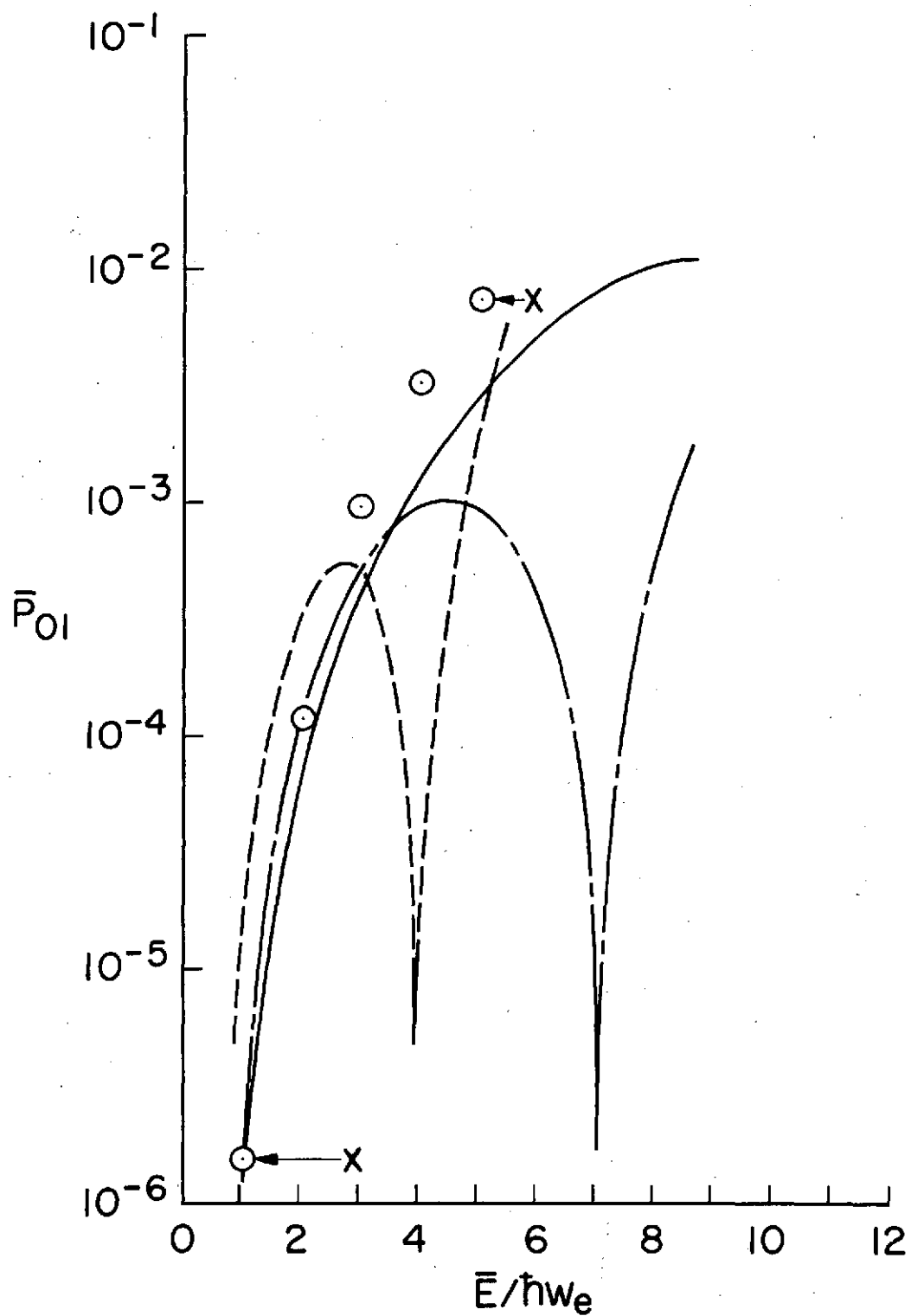


Fig. 3 Comparison of semiclassical and quantum-mechanical transition probabilities for $\text{HBr}(k=0) - \text{He}$ collisions. The impact is between H and He . The notation is the same as in Fig. 2. \circ denotes $k \rightarrow n = 0 \rightarrow 1$.

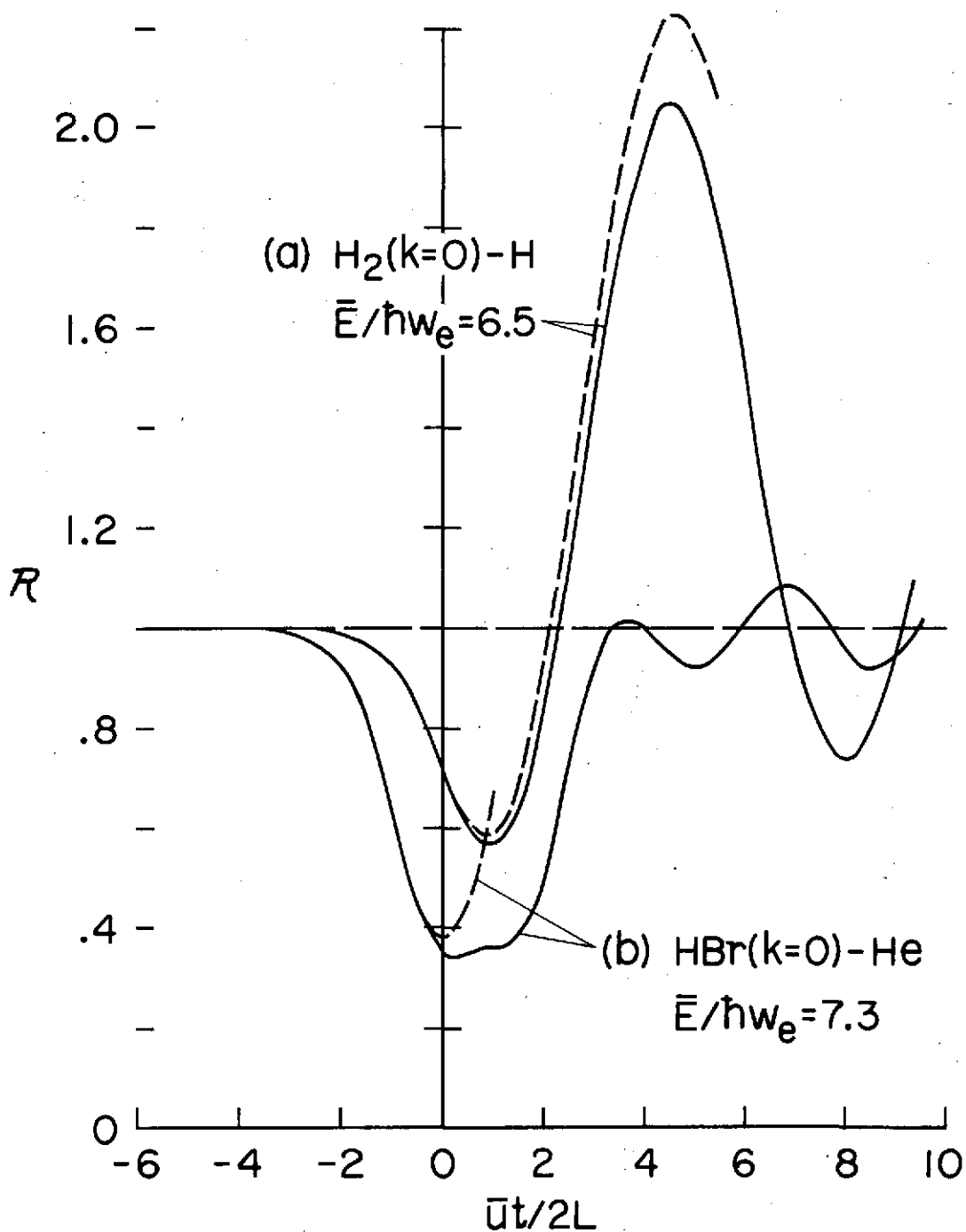


Fig. 4 Transient oscillator effects on the interaction potential. R is defined by Eq. (3b). The curves ——— denote the potential term with the oscillator motion coupled to the classical trajectory. The curves - - - - denote the potential term without coupling.